



Pacific Science Review

NOVEMBER 2008 VOLUME 10 NUMBER 2
Special Issue

*Selected Papers from the 8th Asia-Pacific Conference
on Fundamental Problems of Opto- and Microelectronics
held on September 1~3, 2008 at Kokushikan University, Tokyo, Japan*

Far-Eastern National Technical University, Russia
Kangnam University, Republic of Korea
Harbin Institute of Technology, P.R. China
Kokushikan University, Japan

COHERENT OPTICS AND HOLOGRAPHY

Modulating Wave Holography

O.N. Krokhin.....89

Multichannel Adaptive Interferometer Based on Multiplexed Photorefractive Holograms

R. V. Romashko, Y. N. Kulchin, S. Di Girolamo, A.A. Kamshilin and Han-Young Lee.....93

Characterization of Periodically Poled LiNbO₃ Structures using Digital Holography Microscopy

R.V.Romashko, Hyung-Man Lee, Woo-Seok Yang, Woo-Kyung Kim, Y. Kulchin and Han-Young Lee.....96

OPTICAL METHODS FOR MEASUREMENT AND INFORMATION PROCESSING

A System for Monitoring the Daily Life of the Elderly Based on a Wireless Sensor Network

Seungho Cho and Bonghee Moon.....102

Features of the 1-D Tomography Based upon Single Fiber Multimode Interferometers

Yu.N.Kulchin, O.B.Vitrik and A.D.Lantsov110

Multi-Wavelength Tunable Fiber Ring Laser and its Application to Wavelength-Division Multiplexed Fiber-Bragg Grating Vibration Sensor Array

S. Tanaka, H. Somatomo, N. Takahashi.....113

Combined Time-Wavelength Interrogation of Fiber Bragg Gratings Based on Optical Time-Domain Reflectometry

Yu. N. Kulchin, O.B. Vitrik, A.V. Dyshlyuk, A.M. Shalagin, S.A. Babin, I.S. Shelemba, and A.A. Vlasov117

The Influence of Top-Bottom Close-Proximity Shield Tunneling of a Large Section Captured by Fiber Optic Measurement

N. Horichi, Y. Oku and I. Ono.....121

Design of a Material Surface Defects Detection System Based on FPGA

H. Zhao, Y. Liu, X.-Y. Yu, and Q. Ding.....128

Design of Low Temperature Drift Fiber Fabry-Perot Interferometer Structure based on Finite Element Analysis Method

H. Zhao, X.-Y. Yu, Z. Yue, Q. Ding and Y. Liu.....132

Study on Signal Processing Arithmetic of the FBG Demodulation System Based on the F-P Interferometer

X.-Y. Yu, H. Zhao, Z. Yue, Q. Ding and Y. Liu.....136

Example of Using Small Falling Weight Deflectometer (FWD) for Earth Structures and Low Cost Road Pavement in Japan

H. Shibata, M. Tanaka, I. Ono and T. Okano.....140

Advanced IPTV Technology and Service Deployment

Young-Do Joo.....147

Implementation of an Embedded MVB Protocol Analyzer Sugoog Shon.....	154
Nonlinear Response of Generalized Kubo Oscillator Driven by External Force – A Model of Brain Wave Under Periodic Photo-stimulation – H.Konno.....	160
On Incomplete Pairwise Comparisons in AHP T. Ohya.....	167
Measurement of Plethysmogram and Diagnosis of Stress S. Saito and T. Shimizu.....	170
The Prediction of Plethysmogram by Using the Prediction Method Based on the Mapping Function T. Chikano and T. Shimizu.....	174
The Study on Experiments of Power Current Transformer Based on GMM Y.-L. Xiong, H. Zhao, Z.-G. Bi, L. Wang and W.-L. Yang.....	177
A Study on the Scouring Sensor Based on FBG Jun He, Zhi Zhou, Huijuan Dong, Guangyu Zhang and Jinping Ou.....	182
Study on Coefficient-Adjustable FBG Strain Sensor Packaged with FRP Jun He, Zhi Zhou, Huijuan Dong, Guangyu Zhang and Jinping Ou.....	186
FBG-based Casing Impairment Monitoring in Non-oil Reservoir Jun He, Huijuan Dong, Zhi Zhou, and Guangyu Zhang.....	190
Skeleton-Based Fourier Descriptor of Open Curves E. Tanaka and Y. Tamura.....	194
Non-Gaussian Statistics of Intermittent Chaos in Boussinesq Magnetoconvection N. Bekki, K. Kiyono and H. Konno.....	199
Phase Transitions in Stochastic Systems with Levy-flight Noise M. Shiino and A. Ichiki.....	204
Growth and Characterization of LiAlB₁₄ and NaAlB₁₄ Crystals by Al Self-flux S. Okada, T. Shishido and T. Mori.....	207
<u>NANOTECHNOLOGIES AND NEW MATERIALS FOR OPTOELECTRONICS</u>	
Laser-assisted Nanofabrication Andrei V. Kabashin.....	213
Ultrashort Laser Pulses Induced Metal Surface Micro- and Nanostructures Production: Kynetics of the Crystallization Irina N. Zvestovskaya.....	218
Prospects of Laser Use for Biotechnology A.N. Starodub, and S.D. Zakharov.....	223
Polymer-Based Evanescent Optical Waveguide Bio Sensors H.-Y. Lee, H.-M. Lee, W.-S. Yang, K.-S. Son, S.-S. Lee and W.-K. Kim.....	227

OPTICAL TOPOGRAPHY

Estimation of Partial Optical Path Length for Brain Signal Detected by Near-Infrared Spectroscopy
Y. Niki, W. Matsui and E. Okada.....231

Spatial Resolution of Near Infrared Topography Evaluated by an Adult Head Model
N. Kiryu, H. Kawaguchi and E. Okada.....236

NONLINEAR OPTICS

Representation of Optical Propagation Using Cellular Automata
A. Ankiewicz and Y. Nagai.....241

On the Relationship between Chaotic and Tunnel Ionizations in Strong Optical Fields
Takaaki Onishi.....245

Derivation of a Master Equation for One-photon Emission from an Excited Molecule in a Solvent
K. Umesaki and K. Odai.....248

Investigation of Guided Modes for a Fiber Filled with Chiral Media
Junqing Li and Yusheng Cao.....253

Representation of Optical Propagation Using Cellular Automata

Adrian Ankiewicz* and Yoshinori Nagai **,**

Abstract: Propagation of light in an array of optical guides produces various patterns, depending on whether the material is linear or nonlinear for the power levels used. A parallel array can be used to steer or split light. Our novelty here is to consider discretizing the propagation direction, in addition to the transverse direction. We can then view the linear or nonlinear system in terms of cellular automata for particular 'rules'. This gives an insight into propagation which is different from the continuous approach using differential equations. We give examples and comparisons to make our point.

Keywords: Cellular automata, propagation of light

INTRODUCTION

Light can propagate along parallel discrete optical waveguides [1]. When light with unit power is launched into a central waveguide (labeled $n=0$), competing effects influence the propagation. Even for linear materials, light can couple to the 2 neighboring guides $n = \pm 1$, thus decreasing the central intensity. In turn, each of these can couple to its near neighbors and so the light spreads out or 'diffracts' with propagation distance, z . The coupling involves the 2 neighbors and so can be described by $A_{n+1}(z) - A_{n-1}(z)$, or after another iteration, by $A_{n+1}(z) + A_{n-1}(z) - 2A_n(z)$. This is the discrete version of a second derivative evaluated at node n . So the basic equation is

$$i \frac{dA_n(z)}{dz} + c(A_{n+1}(z) + A_{n-1}(z)) = 0. \quad (1)$$

By noting the recurrence relations for the Bessel function of the first kind (J), we can easily see that the amplitude for guide n evolves as $A_n(z) = i^n J_n(2cz)$, where c is the coupling coefficient between guides [1,2]. Thus the power in guide n is $J_n^2(2cz)$.

If there is no material attenuation in the system, then conservation of energy is easily verified by observing

$$\text{that } P(z) = \sum_{n=-\infty}^{\infty} |A_n|^2 = \sum_{n=-\infty}^{\infty} J_n^2(2cz) = 1.$$

An example of this propagation is given in fig.1. Various conservation laws also exist for cellular automata (CA). The Bessel functions take the forms of decaying sinusoids when the argument is not too small. We will use this periodicity to demonstrate a simple CA representation of the linear optical array later in section 3(a).

PROPAGATION IN ARRAY OPTICAL WAVEGUIDES

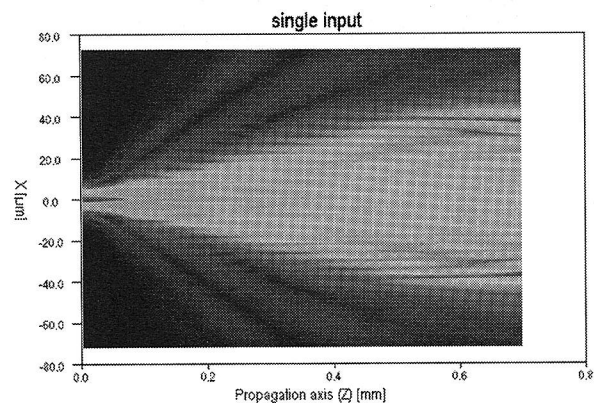


Fig.1. Example of power being distributed to various guides from a single input. The central part clearly resembles the triangular chess-board discussed in the CA description in part 3(a) and presented with the matrix B.

If we use 2 or more inputs, then we can use unequal initial phases to tilt the propagating beam. For example, Fig.2 has 3 inputs, each of unit power, but the phase of

* Optical Sciences Centre,

** Applied Mathematics Dept.,

Research School of Physical Sciences and Engineering, Australian National University, Canberra, ACT 0200.

*** Centre for Information Science and School of Political and Economic Sciences, Kokushikan University, 4-28-1 Setagaya, Tokyo, 154-8515, Japan.

the upper input is +90 degrees relative to the central one, and the phase of the lower guide is -90 degrees relative to the central one. As a result, the system acts like a radar phased array and the beam is directed upwards.

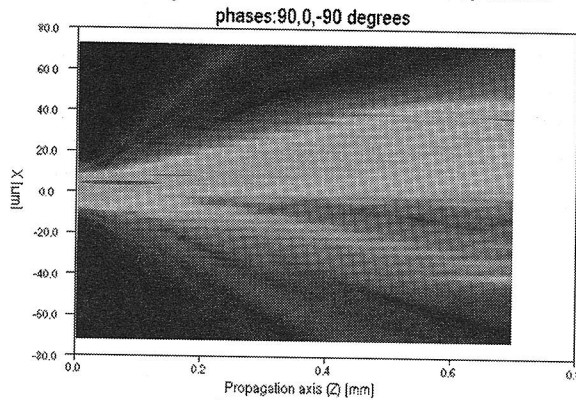


Fig.2. Beam tilts upwards due to initial phase ramp.

In Fig.3 there are also 3 inputs, each of unit power, but the phase of the upper input is -90 degrees relative to the central one, and the phase of the lower guide is +90 degrees relative to the central one. As a result, the beam is directed downwards.

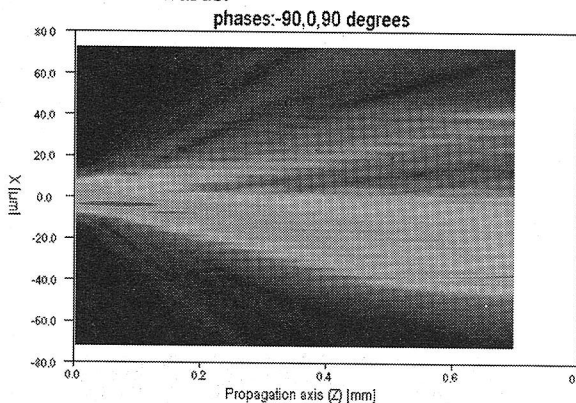


Fig.3 Beam tilts downwards due to initial phase ramp.

This spreading can be suppressed if the material is nonlinear, since there is an increment in refractive index which is proportional to the local light intensity. To account for this, we add a cubic term to the basic equation and arrive at an Ablowitz-Ladik-type equation [3]:

$$i \frac{dA_n(z)}{dz} + c(A_{n+1}(z) + A_{n-1}(z)) + k |A_n(z)|^2 A_n(z) = 0.$$

This is clearly a discrete version of the nonlinear Schrodinger equation [5], and other terms can be added to describe various effects. It has been shown that this system supports front-like and quasi-rectangular (bright, flat-top) solitons [3]. Since the transition region (from '0' to '1') is very narrow, we can speculate that it may be possible to use an even simpler model. In this conference paper, we use cellular automata to investigate this

possibility.

In an earlier paper [4], we explained some principles of a matrix approach to cellular automata, and showed that soliton-type effects, such as fusion and elastic collisions, are possible for some cellular automata with quite simple nonlinear evolution rules. We also demonstrated a simple way of constructing such CA. Certain forms can be used to represent optical solitons.

The use of spatial solitons brings the chance of steering solitons [6] and making optical networks which can be adapted in configuration as the need arises [7].

USING CELLULAR AUTOMATA TO REPRESENT DISCRETE SOLITONS

(a) Linear propagation.

In section 1, we considered continuous solutions of eq.1. Now the asymptotic form of the J Bessel function is

$$J_n(z) \approx \sqrt{\frac{2}{\pi z}} \cos\left(z - \frac{n\pi}{2} - \frac{\pi}{4}\right),$$

so we set the discretized propagation distance to be

$$z_m = \frac{\pi}{8c}(1 + 2m) \text{ for } m=0,1,2,\dots, \text{ This is accurate for}$$

$|n| < m$, so we limit ourselves to this range. Then we find that the amplitude in guide n at distance corresponding to m will be

$$A_n(z_m) \approx 2 \frac{i^n}{\pi} \sqrt{\frac{1}{m + \frac{1}{2}}} \cos\left(\frac{m-n}{2}\pi\right) = 2 \frac{i^n}{\pi} \sqrt{\frac{1}{m + \frac{1}{2}}} \frac{1}{2} (i^{m-n} + i^{n-m}).$$

We define the normalized amplitude to be

$$B_n^m = \frac{1}{2} \pi \sqrt{m + \frac{1}{2}} A_n(z_m) = \frac{1}{2} (i^m + i^{2n-m}), -m \leq n \leq m.$$

For iteration m , we find that $2m+1$ sites are occupied, with almost half being zero. Hence the power in the central region,

$$P(z) = \sum_{n=-m}^m |A_n(z_m)|^2 \approx \frac{4}{\pi^2} \text{ remains constant on}$$

propagation and so even this rough calculation shows the conservation of energy. Thus the intensity pattern resembles an expanding chess-board with triangular sides, as we have allowed for the $1/m$ decrease in intensity for sites with label m . Here is the matrix $B[n,m]$ which gives the evolution of amplitude for small values of m from $m=0$ to $m=6$ for $-5 \leq n \leq 5$:

$$B = \begin{pmatrix} 0 & 0 & 0 & 0 & 0 & 1 & 0 & 0 & 0 & 0 & 0 \\ 0 & 0 & 0 & 0 & i & 0 & i & 0 & 0 & 0 & 0 \\ 0 & 0 & 0 & -1 & 0 & -1 & 0 & -1 & 0 & 0 & 0 \\ 0 & 0 & -i & 0 & -i & 0 & -i & 0 & -i & 0 & 0 \\ 0 & 1 & 0 & 1 & 0 & 1 & 0 & 1 & 0 & 1 & 0 \\ i & 0 & i & 0 & i & 0 & i & 0 & i & 0 & i \end{pmatrix}$$

Hence there is a phase advance of 90 degrees with each increment in m (i.e. $1 \rightarrow i \rightarrow -1 \rightarrow -i \rightarrow 1$), and a guide always has amplitude 0 if it had power in the previous iteration. Clearly, B corresponds to a CA system with a simple rule involving the site and its 2 nearest neighbors only.

We now investigate this rule using the formalism described in section 3 of our earlier work [4]. Clearly this is a case with 5 levels, viz. $\{0, i, -1, -i, 1\}$, so $L=5$. The element occurring at position (j, k) depends on 3 factors, namely $a=m(j-1, k-1)$, $b=m(j-1, k)$ and $c=m(j-1, k+1)$, so $N=3$. We expect a rule which is symmetric for the swapping of elements 'a' and 'c'. We find that

$$f(a, b, c) = \frac{i}{4} (b^4 - 1)(a + c) [ac(3a^2 - 4ac + 3c^2) - 4]$$

This is indeed symmetric with respect to $a \leftrightarrow c$. Also, if b is non-zero, then the element below it will be zero, hence creating the chess-board pattern. The vector x has $5^3 = 125$ elements. We find that

$$x_2 = i, x_{22} = -i, x_{26} = i, x_{30} = -3i/4, x_{46} = -i, x_{50} = 3i/4, x_{54} = i/4, x_{74} = -i/4$$

while

$$x_{78} = i/4, x_{98} = -i/4, x_{102} = -3i/4, x_{122} = 3i/4.$$

The remaining elements are zero.

Here is a color representation of B:

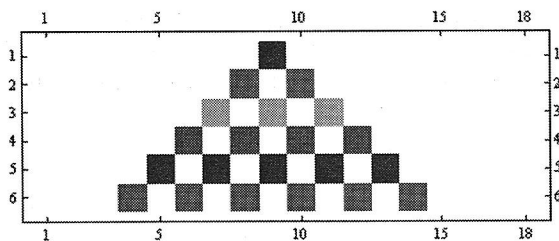


Fig.4. Evolution of CA for matrix B. Here blue=1, red=i, green=-1, purple=-i and white=0. See right hand side of fig.1. Clearly this resembles the propagation in fig.1 (rotated 90°).

(b) Nonlinear effects

Various terms can be added to the basic equation to allow for higher-order nonlinearity and gain/loss in the system [8]. Direct simulations can be used to solve these array systems and even get some analytic results [9]. However, our aim here is rather different. We seek the simplest models which can represent the interaction, collision and repulsion of solitons. We give some examples. Two solitons can merge and form a different soliton, as shown in fig.5. Solitons moving left and right collide with each other and pass through each other, suffering only a lateral shift [5]. Here the CA in figs. 6 and 7 also show this feature. In each case, the lateral shift is one unit. The behavior close to the collision site differs in each case, whereas the behavior far from this point is the same. This also occurred in the optical case [e.g. see page 115 of ref.5]. The central rectangular-type soliton which we discussed in the introduction is represented by two or more '1's in a row [see fig.8 below]. Figs. 5, 6 and 7 all use the same rule form for f , namely:

$$f = 1/8 (a^2 (-2 (1+b) (2+b) + (-4+b (3+5 b)) c) + (4+b (11+b)) c^2 - 2 (2 (-1+c) c + b^2 (-1+c) (4+c) + b c (1+3 c)) + a (4+b (-2+3 c (1+c) + b (-6+(-3+c) c))))).$$

The vector x is:

$$\{\{0\}, \{1/2\}, \{-1/2\}, \{0\}, \{-1/4\}, \{-3/4\}, \{1\}, \{-3/4\}, \{-1/4\}, \{1/2\}, \{0\}, \{-1/2\}, \{-1/4\}, \{3/8\}, \{3/8\}, \{-3/4\}, \{-3/8\}, \{5/8\}, \{-1/2\}, \{0\}, \{1/2\}, \{-3/4\}, \{3/8\}, \{11/8\}, \{-1/4\}, \{1/8\}, \{1/8\}\}.$$

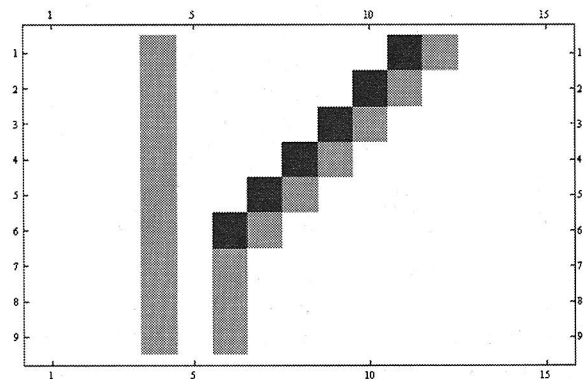


Fig.5. Fusion of unit $\{0,1,0\}$ soliton with $L=\{-1,1\}$ to form $\{1,0,1\}$ soliton.

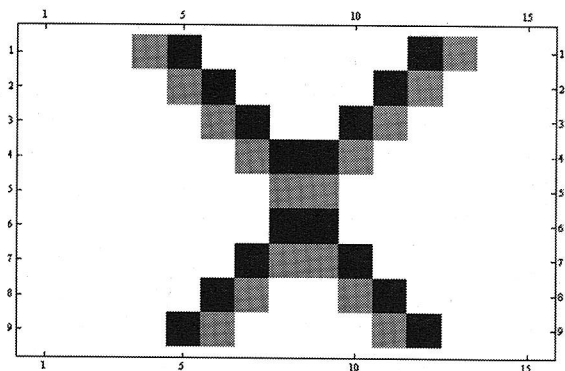


Fig 6. Solitons collide, with even number of zeros between them at start. Here 1 is indicated in green, -1 with blue and 0 with white. The collision is lossless, and the solitons pass through each other with only a lateral shift of one space. See eq.30 of [4].

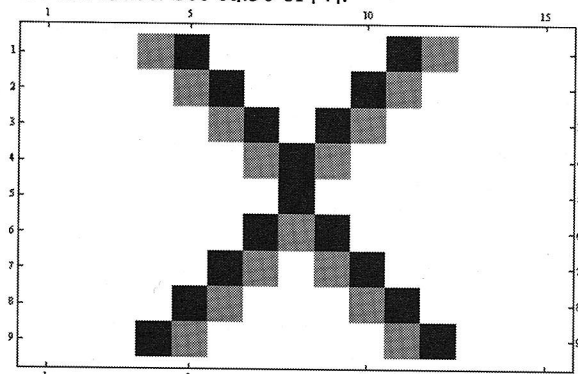


Fig.7. Solitons collide, with odd number of zeros between them at start. See eq.29 of [4]. Green=1, blue=-1, white=0.

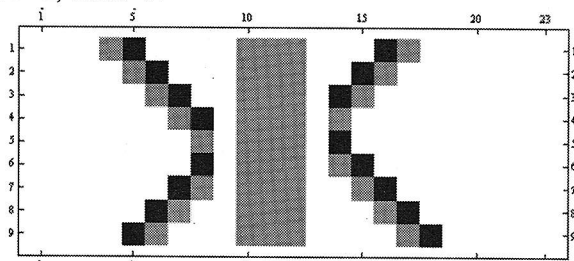


Fig.8. Reflections off a rectangular soliton—signal reflected by ‘blocker’—see fig.10 of [10] and fig.4 of [11]. Here green=1 and blue=-1 and white=0. So the right-moving soliton, R, is $\{+1,-1\}$ while the left-moving soliton, L, is $\{-1,+1\}$.

In fig.8, we have used a different rule: $f=1/2 (a-(-1+c) c - a^2 c^2 + 2 b^2 c^2 + 2 b (-1+c^2) - a^2 (1-2 b+c-2 c^2+b^2 (-2+4 c^2)))$. Clearly, the L soliton, which consists of the set $\{-1,+1\}$ is effectively a phase ramp, and this produces the motion (to the left). Similarly, the R soliton, which consists of the set $\{+1,-1\}$ is also a phase ramp, and it moves to the right. The correspondence of L and R with figures 2 and 3 is clear.

CONCLUSIONS

We have provided simulations of optical propagation in an array and showed up analogies between these simulations and the cellular automata appearing due to iterated behavior. In the first case, the propagation variable (z) is continuous, whereas the iterations in CA are plainly discrete. Hence it is fascinating to see the connection between the two. The CA may be used to gain insight into linear and nonlinear optical propagation in waveguides.

REFERENCES

- [1] S. Somekh et al., *Appl. Phys. Lett.*, 22,(1973), 46.
- [2] M.C.Gabriel and N.Whitaker, *J.Lightwave Tech.*, 7,(1989), 1343.
- [3] S.Darmanyan, A.Kobyuakov, F.Lederer and L.Vazquez, "Discrete fronts and quasi-rectangular solitons", *Phys.Rev. B*, 59,(1999),5994-7.
- [4] Adrian Ankiewicz and Yoshinori Nagai, 'Solitons in multi-level cellular automata', *Chaos, solitons & fractals*. 13,(2002),1345-58.
- [5] N. Akhmediev and A.Ankiewicz, *Solitons: nonlinear pulses and beams*, [Chapman and Hall, London, 1997].
- [6] Stephen R. Friberg, "Soliton fusion and steering by the simultaneous launch of two different-color solitons", *Optics Lett.*, 16,(1991),1484-1486.
- [7] Z.Xu et al., 'Reconfigurable soliton networks optically-induced by arrays of non-diffracting Bessel beams', *Optics Express*, 13 (2005)1774.
- [8] J. M. Soto-Crespo, Nail Akhmediev and A. Ankiewicz, 'Motion and Stability Properties of Solitons in Discrete Dissipative Structures', *Phys.Lett A.*, 314, (2003) 126-130.
- [9] Ken-ichi Maruno, Adrian Ankiewicz and Nail Akhmediev, 'Dissipative solitons of the discrete complex cubic-quintic Ginzburg-Landau equation', *Physics Letters A*, 347, (2005), 231-240.
- [10] J.Meier et al, *Optics Express*, 13, 1797, (2005).
- [11] E.Smirmov et al., *Optics Express*, 14, 11248-55, (2006).